JOURNAL OF CATALYSIS 135, 335–344 (1992)

Oxidation of NH_3 over $YBa_2Cu_3O_7$(123) Oxide Systems[1]

S. RAMESH AND M. S. HEGDE[2]

Solid State and Structural Chemistry Unit, Indian Institute of Science, Bangalore 560 012, India

Received March 18, 1991; revised August 30, 1991

A temperature-programmed desorption study showed that the activation energy of oxygen desorption from $YBa_2Cu_3O_{7-x}$ ($x = 0.05$), $PrBa_2Cu_3O_{7-x}$ ($x = 0.02$), and $YBa_2Cu_2CoO_{7+x}$ ($x = 0.26$) were 28.2, 26.4, and 22.3 kcal/mole, respectively. Anaerobic oxidation of NH_3 over these oxide systems shows the formation of H_2O, N_2, and NO transforming the oxides to tetragonal phases. Aerobic oxidation of NH_3 is NO specific over all the three oxide catalysts. The Co-substituted $YBa_2Cu_2CoO_{7+x}$ was the most reactive and stable oxide in this family; the lower oxygen desorption energy and higher reactivity are suggested to be due to the presence of holes in the form $Co^{4+}O^{2-} \rightleftarrows Co^{3+}O^-$. The conversion of NH_3 to NO was nearly 100% above 400°C when the ammonia flow rates were 10 μmole/cm^2/s over 0.3 g of the $YBa_2Cu_2CoO_{7+x}$ catalyst.

INTRODUCTION

$YBa_2Cu_3O_{7-x}$(123) is a much studied oxide system since its discovery as a superconducting oxide (*1*). Fully oxygenated 123 has orthorhombic structure (123(O)). Oxygen desorption from this compound leads to $YBa_2Cu_3O_{6.4}$(123(T)) with a tetragonal structure and the compound is semiconducting (*2–4*). The heat of desorption of oxygen from 123(O) to 123(T) is about 27 kcal/mole (*5*), which is lower than the oxygen desorption energy from Ag/O_2 and Pt/O_2 systems (*6*). It is also known from thermogravimetric study that the temperature at which oxygen desorption occurs increases with the increase of x in $YBa_2Cu_3O_{7-x}$, indicating that the labile oxygen in this system is dissociated (atomic) oxygen. Therefore, 123(O) is expected to act as an oxidation catalyst. Having seen the availability of labile oxygen, several catalytic studies have been carried out. Hansen *et al.* (*7*) were the first to employ $YBa_2Cu_3O_{6+x}$(123(T)) as an ammoxidation catalyst, viz., oxidation of toluene to benzonitrile. Subsequently, Salvador (*8*) showed quantitative oxidation of CH_4 to CO_2 and H_2O over 123(O). However, CO_2 was readsorbed by the compound to form $BaCO_3$. To that extent, the compound was decomposed. Stationary catalytic reaction $NO + CO \rightarrow N_2 + CO_2$ was shown to occur on 123(T) (*9*). Oxidation of CO to CO_2 has also been shown on other insulating ternary Cu oxides (*10*). The studies on 123 as a catalyst were restricted to $YBa_2Cu_3O_7$(O) and $YBa_2Cu_3O_{6+x}$(T).

Electrical conductivity, structure and oxygen content are interrelated in the case of 123. As the oxygen in $YBa_2Cu_3O_{6.4}$(123(T)) is increased, the compound becomes orthorhombic and also becomes metallic and superconducting. Conductivity at 300 K increases with increase in oxygen content. Furthermore, the superconducting transition temperature increases from 0 to 90 K for increase in oxygen content from $O_{6.4}$ to $O_{6.95}$. Simultaneously, the onset temperature for oxygen desorption decreases from 550 to 350°C with the increase in oxygen content (*5*). Thus, conductivity of 123 does give information on the availability of labile oxygen. The electrical conductivity behavior of 123 can be altered by cationic substitution. For example, yittrium can be substi-

[1] Contribution No. 759 from the Solid State and Structural Chemistry Unit.

[2] To whom correspondence should be addressed.

0021-9517/92 $5.00

tuted by praseodymium keeping the compound orthorhombic ($PrBa_2Cu_3O_7$), but it is semiconducting (*11*). $YBa_2Cu_2CoO_{7\pm x}$ has been synthesized, wherein the Co^{3+} ion occupies the chain Cu position and this compound is insulating (*12*). Weight loss due to oxygen desorption from this compound has been observed (*12*). Similarly, oxygen desorption from Pr123 has also been observed (*13*). The question is whether the oxygen from the semiconducting and the insulating compounds of the 123 family is more or less reactive than that of the $YBa_2Cu_3O_{7-x}$ itself. Such substitutions also bring about a decrease in the positive hole concentration, simultaneously making the compound nonsuperconducting (*12*). Reactivity of oxygen in such substituted 123 may decrease since the holes are known to be in the oxygen ion. We have therefore undertaken a study of 123 as an oxidation catalyst specifically to identify the reactive oxygen in the 123 system. It seems possible to selectively vary the binding energy of the labile oxygen through cationic substitution. In this study, we report on the oxygen chemistry of $YBa_2Cu_3O_{7-x}$(123), $PrBa_2Cu_3O_{7-y}$(Pr123), and $YBa_2Cu_2CoO_{7\pm x}$(1221), employing temperature-programmed desorption (TPD) and temperature-programmed reaction (TPR) techniques. NH_3 oxidation under anaerobic and aerobic conditions has been employed as a test reaction. The results are supported by structural studies on the catalyst before and after the reaction.

EXPERIMENTAL

123, Pr123, and 1221 oxides were synthesized by heating stoichiometric mixtures of Y_2O_3, BaO_2, CuO, Pr_6O_{11}, and $Co(C_2O_4) \cdot 2H_2O$ at 930°C for 60 h with three intermittent grindings. The oxides were then cooled from 900 to 30°C in oxygen at a rate of 1°C per min. Sample purity was checked by X-ray diffraction using Cu$K\alpha$ radiation employing a Jeol X-ray diffractometer. Cell parameters of all the oxides were in agreement with the values reported in the literature (*12–14*). We have also synthesized $Y_{1-x}Pr_xBa_2Cu_3O_{7-y}$ as well as $YBa_2Cu_{3-x}Co_xO_{7+y}$ ($0 < x < 1$). Since the variation in the reactivity of oxygen was small, only the end members of these two oxide series have been fully examined for their catalytic activity. The 123(O) was superconducting with T_c of 90 K. Oxygen content was estimated from iodometric titration (*15*) and the oxygen in the formula is accurate within ±0.04. In each case, the well-sintered pellets were finely powdered and the surface areas were determined using a Cilas-Alcatel 715E granulometer. The surface areas were in the range of 0.1 to 0.2 m^2/g.

Temperature-programmed reaction/desorption was carried out in a 6-mm-diam quartz continuous flow reactor. The reactor tube was pumped to 10^{-6} Torr by a diffusion pump. The evolved gas was sampled through a fine control leak valve to a UHV system housing a Vacuum Generators quadrupole mass spectrometer at 10^{-9} Torr. The gas sampling was performed every 10 s over the period of the experiment. The sample temperature was measured by immersing a fine chromel–alumel thermocouple into the catalyst, and the mass signal and the temperature sensed from the thermocouple were fed to an A/D converter and the digitised signals were acquired by a PC/AT.

A typical experiment carried out here is as follows. Finely powdered 0.3 g of the oxide was loaded into the reactor and pumped to 10^{-6} Torr. The sample was heated at 15°C/min from 30 to 650°C. At the interval of a 3°C rise in temperature, gas analysis was carried out. At the end of a run, which is typically 225 scans, peak height of each mass and the corresponding temperature were retrieved and the thermograms were generated. In the case of reactions, gases such as NH_3, $NH_3 + O_2$ were passed over the catalyst at a constant flow rate with 15°C/min heating rate. Flow rate of ammonia was generally 8 μmole/cm^2/s and it was varied from 2 to 15 μmole/cm^2/s.

RESULTS AND DISCUSSION

Oxygen desorption thermograms for the 123, Pr123, and 1221 oxides are shown in

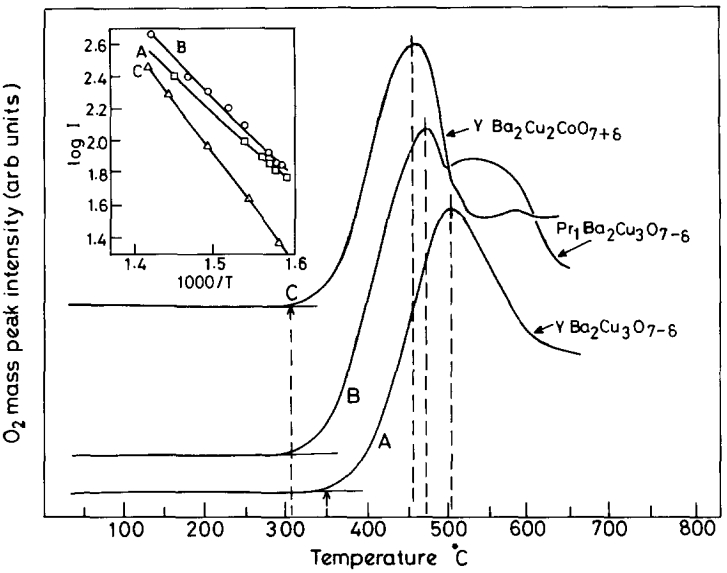

FIG. 1. Temperature-programmed desorption of oxygen from (A) 123, (B) Pr123, and (C) 1221. Inset shows Arrhenius or Polanyi–Wigner plots for oxygen desorption.

Fig. 1. When these oxides are exposed to air, they absorb H_2O and CO_2. Adsorbed CO_2 reacts with the compounds forming $BaCO_3$. TPD of the air-exposed oxides gave H_2O and CO_2 in addition to oxygen. However, desorption of H_2O, CO_2, and CO were not observed during this study, indicating that the compounds were pure. Onset temperature for oxygen desorption was 310°C for the Co-substituted 1221 oxide and 350°C for 123. The peak temperature of oxygen desorption was 450°C for the 1221 and 500°C in the case of 123. The peak temperature of oxygen desorption was 470°C in the case

TABLE 1

The Variation of Cell Parameters and Cell Volume in the $YBa_2Cu_3O_{7-x}$ System

Sl. No.	System	Structure[a]	a (Å)	b (Å)	c (Å)	V^b (Å^3)	Oxygen content[c]
1.	$YBa_2Cu_3O_{6.95}$	O	3.81	3.89	11.65	172.66	6.95
2.	$YBa_2Cu_3O_{6.42}$ (oxygen desorbed)	T	3.88	—	11.70	176.13	6.42
3.	$YBa_2Cu_3O_{7-x}/NH_3$ TPR/30-650 C	T	3.92	—	11.75	180.55	6.35
4.	$YBa_2Cu_3O_{7-x}/NH_3$/ Iso thermal (370 C)	T	3.87	—	11.74	175.82	6.46
5.	$YBa_2Cu_3O_{7-x}/NH_3 + O_2$/ 1 : 5/TPR/30–650°C	O	3.82	3.88	11.66	172.81	6.78
6.	$YBa_2Cu_3O_{6+x}/NH_3 + O_2$/TPR	O	3.82	3.89	11.71	173.56	6.65

[a] O, orthorhombic; T, tetragonal.
[b] Cell volume.
[c] Oxygen content given here is accurate within ±0.04.

TABLE 2

The Variation of Cell Parameters and Cell Volume in the $PrBa_2Cu_3O_{7-x}$ Systems[a]

Sl. No.	Systems	Structure	a (Å)	b (Å)	c (Å)	V (Å^3)	Oxygen content
1.	$PrBa_2Cu_3O_{6.98}$	O	3.86	3.91	11.71	176.73	6.98
2.	$PrBa_2Cu_3O_{6+x}$ (oxygen desorbed)	T	3.92	—	11.78	181.01	6.60
3.	$PrBa_2Cu_3O_{7-x}/NH_3$/TPR/30–650/15°C/min	T	3.92	—	11.77	180.24	6.56
4.	$PrBa_2Cu_3O_{7-x}/NH_3$/isothermal/370°C	T	3.92	—	11.7	180.24	6.59
5.	$PrBa_2Cu_3O_{7-x}/NH_3 + O_2$/TPR product	T	3.91	—	11.80	180.39	6.46
6.	$PrBa_2Cu_3O_{6+x}/NH_3 + O_2$/TPR product	T	3.92	—	11.74	180.40	6.46

[a] See the footnotes for Table 1.

of Pr123. The activation energy determined from Arrhenius (or Polanyi–Wigner) plots (*16*) were 22.3, 26.4, and 28.2 kcal/mole for 1221, Pr123, and 123, respectively. These values could be reproduced within ±1.5 kcal/mole. Cell parameters of these oxides before and after oxygen desorption (up to 650°C) are given in Tables 1–3. The increase in the cell volume for 123 and Pr123 after oxygen desorption is by about 3 Å^3 and it matches well with the values reported in the literature (*12–14*). Furthermore, a linear increase in c-axis with decrease in oxygen content, i.e., with x in $YBa_2Cu_3O_{7-x}$ and the corresponding Pr123, has been observed as expected. However, the variation in the c parameter with x was not significant in the case of 1221. 123 and Pr123 oxides transform from orthorhombic to tetragonal structure. The Co-substituted 1221 remains tetragonal before and after oxygen desorption. Oxygen estimation by the iodometric titration method showed that $YBa_2Cu_3O_{6.95}$ upon oxygen desorption goes to $YBa_2Cu_3O_{6.45}$; $PrBa_2Cu_3O_{6.98}$ goes to $PrBa_2Cu_3O_{6.6}$; and $YBa_2Cu_2CoO_{7.26}$ goes to $YBa_2Cu_2CoO_{7.14}$. Thus, the amounts of oxygen desorbed per mole of the oxide vary in the ratio 1 : 0.76 : 0.25 for 123, Pr123, and 1221, respectively. Alternatively, the quantity of oxygen desorbed from these three systems obtained from the area under the oxygen desorption curve was found to vary as 1 : 0.77 : 0.3, which is close to the ratio obtained from the titration. It is also important to note that in the case of the co-substituted compound, excess over O_7 is desorbed. Furthermore, the decrease in oxygen content

TABLE 3

The Variation of Cell Parameters and Cell Volume in the $YBa_2Cu_2CoO_{7+x}$ Systems[a]

Sl. No.	System	Structure	a (Å)	b (Å)	c (Å)	V (Å^3)	Oxygen content
1.	$YBa_2Cu_2CoO_{7+x}$	T	3.88	—	11.66	175.53	7.26
2.	$YBa_2Cu_2O_{7+x}$ oxygen desorbed	T	3.88	—	11.68	175.83	7.14
3.	$YBa_2Cu_2CoO_{7+x}/NH_3$	T	3.88	—	11.66	175.53	7.02
4.	$YBa_2Cu_2CoO_{7+x}/NH_3$ isothermal/370°C	T	3.89	—	11.66	176.44	7.07
5.	$YBa_2Cu_2CoO_{7+x}/(NH_3 + O_2)$/1 : 5	T	3.89	—	11.67	176.59	7.17
6.	$YBa_2Cu_2CoO_{7+x}$/desorbed/$NH_3 + O_2$/1 : 5/TPR	T	3.88	—	11.71	176.28	7.11

[a] See the footnotes for Table 1.

upon oxygen desorption is lowest in the case of 1221.

The activation energy of oxygen desorption from 123(T) is about 54 kcal/mole (*5*), which is much higher than that from 123(O) with a value of 28 kcal/mole. Also, the onset temperature of oxygen desorption is higher for 123(T) than for 123(O). Such behaviour in 123 can be explained by considering the fact that as the oxygen content in 123(T) is increased to form 123(O), there is an increase in the hole concentration. Holes are considered to be present on both Cu and oxygen in 123 as given by (*17*).

$$Cu^{3+}O^{2-} \rightleftarrows Cu^{2+}O^{-}. \qquad (1)$$

Although the dissociation of a metal oxide is written by a simple chemical reaction,

$$M^{2+}O^{2-} \rightarrow M + \tfrac{1}{2}O_2(g) - \Delta H, \qquad (2)$$

several steps are involved in this reaction. Oxygen desorption from an oxide should follow the sequence (*18*)

$$O^{2-} \xrightarrow[-\Delta H_1]{-e} O^{-} \xrightarrow[-\Delta H_2]{-e} O\,(ad) \xrightarrow[-\Delta H_3]{} \tfrac{1}{2}O_2\,(ad) \xrightarrow[-\Delta H4]{} \tfrac{1}{2}O_2\,(g). \qquad (3)$$

Each step in this sequence of reactions involves finite energy and ΔH of total reaction (2) is the sum of the individual reactions (*18*). If there are holes in oxygen in an oxide, meaning thereby the presence of O^--like ions as represented in Eq. (1), the oxygen desorption energy should be lower by a fraction of ΔH_1 compared to the charge-balanced oxide containing O^{2-}-like ions. When the hole concentration is increased, an increase in O^- as per Eq. (1) occurs, leading to a lower desorption energy.

The purpose of studying oxygen desorption of Pr123 was to see if labile oxygen is more strongly bound compared to the 123(O) because it is known that the hole concentration responsible for the metallic and superconducting property is decreased due to Pr ion substitution in place of the Y ion. The same is true of Co ion substitution in the chain Cu position. The activation energy of oxygen desorption in Pr123 is lower than that of 123(O), contrary to expectation. Therefore the binding energy of the labile oxygen associated with the chain Cu is not altered in the case of Pr123.

The Co-substituted 1221 is an interesting compound. The oxygen desorption energy is lower than that in 123, indicating that the labile oxygen is not more strongly bound due to the presence of Co^{3+} ion in the chain Cu position. The total oxygen in the oxygen-annealed sample is 7.26, which agrees well with the values reported in the literature (*12, 19*). In 123, the presence of holes is well recognised and the bond valence study shows that the Cu valence is intermediate between +2 and +3 (*20*). Taking the formal valencies of ions as Y^{3+}, Ba^{2+}, Cu^{2+}, Co^{3+}, and O^{2-}, $YBa_2Cu_2CoO_7$ forms a stoichiometric compound. This implies that there are 0.52 holes in the oxygenated $YBa_2Cu_2CoO_{7.26}$ compound. This means that either part of Cu is oxidised to +3 or Co is oxidised to +4 valence states. It is reasonably understood from the neutron diffraction studies that the Co^{3+} ion occupies the chain Cu position and since Co^{3+} is stable in octahedral coordination, the extra oxygen should be in the *a*/2 lattice position (*21*). Charge balancing in $YBa_2Cu_2CoO_{7.25}$ can be achieved in two ways: (a) $Y^{3+}Ba_2^{2+}Cu_2^{2.25+}Co^{3+}O_{7.25}^{2-}$, indicating that part of Cu is oxidised to the Cu^{3+} state, and (b) $Y^{3+}Ba_2^{2+}Cu_2^{2+}Co^{3.5+}O_{7.25}^{2-}$, indicating that half of the Co is in +3 and half is in +4 oxidation states. It is known that with 0.25 holes per plane Cu in the cuprates, the compound is expected to be metallic and superconducting (*22*). However, this compound is semiconducting. Therefore it is unlikely that Cu is oxidised to +3 state or the holes are residing in the Cu–O_2 sheets in 1221, unlike in 123. Alternatively, part of Co^{3+} can be oxidised to Co^{4+}. The low oxygen desorption energy in this compound can then be due to holes that can be represented as

$$CO^{4+}O^{2-} \rightleftarrows Co^{3+}O^{-}. \qquad (4)$$

The oxygen desorption temperature of

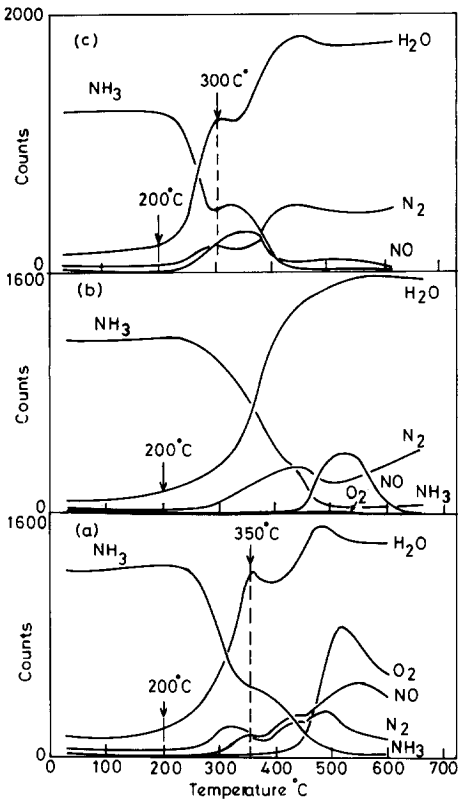

FIG. 2. Thermograms of anaerobic ammonia oxidation over (a) 123, (b) Pr123, and (c) 1221. The oxides used here were fully oxygenated. Flow rate of ammonia was 8 μmole/cm^2/s.

this compound compares well with $La_{1-x}Sr_xCoO_3$ (*23*); and, therefore, the oxygen reactivity in the Co-substituted 1221 is suggested to be due to the oxygen associated with Co.

Anaerobic Oxidation of NH_3

NH_3 gas was passed over 0.3 g of the oxides and the products were analysed over a temperature range of 30–650°C. The thermograms of NH_3 over 123, Pr123, and 1221 are shown in Figs. 2a, 2b, and 2c, respectively. H_2O, N_2, and NO were the products. In the case of 123 and Pr123, O_2 was also desorbed. Onset temperature of H_2O formation from the hydrogen abstraction reaction from NH_3 was about 200°C in all the cases. It must be noted that at the temperature at which O_2 desorption occurred, mainly NO and H_2O were formed (see Figs. 2a and 2b). Furthermore, the peak temperature of NO formation was lowest at 350°C in the case of 1221 followed by Pr123 and 123 at 500°C. Formation of NO at a lower temperature in the case of 1221 correlates well with the lower oxygen desorption temperature of this compound. Figure 3 shows the thermograms for NH_3 over oxygen-desorbed 123 showing only N_2 and H_2O formation above 500°C. At the end of the run, the compound was decomposed to basic oxides indicating that ammonia acts as a reducing agent. However, the oxygen-annealed 1221 and 123 did not show decomposition of the oxides to basic oxides in a run up to 650°C, but the Pr123 showed a slight decomposition to Cu_2O and other basic oxides. This then shows that $PrBa_2Cu_3O_7$ is less stable to NH_3. We have also carried out isothermal reaction with NH_3 at 370°C; in the case of 123 and Pr123, H_2O and N_2 were the main products. NH_3 over 1221 at 370°C gave NO as well and the compound was stable enough to give $YBa_2Cu_2CoO_{7.02}$. Thus, holes in 1221 can be selectively removed by employing NH_3 as a reducing agent. Lattice parameters and oxygen content obtained before and after the reactions are given in Tables 1–3.

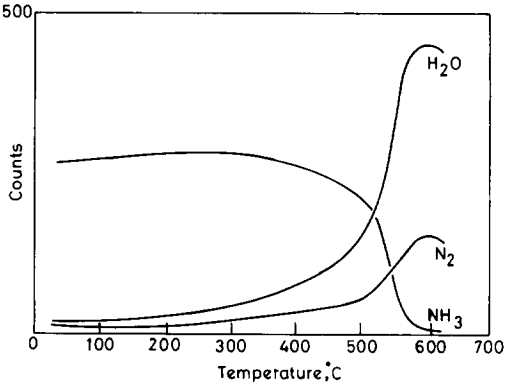

FIG. 3. Thermograms of anaerobic oxidation over oxygen-desorbed 123 for the same flow rate as that in Fig. 2.

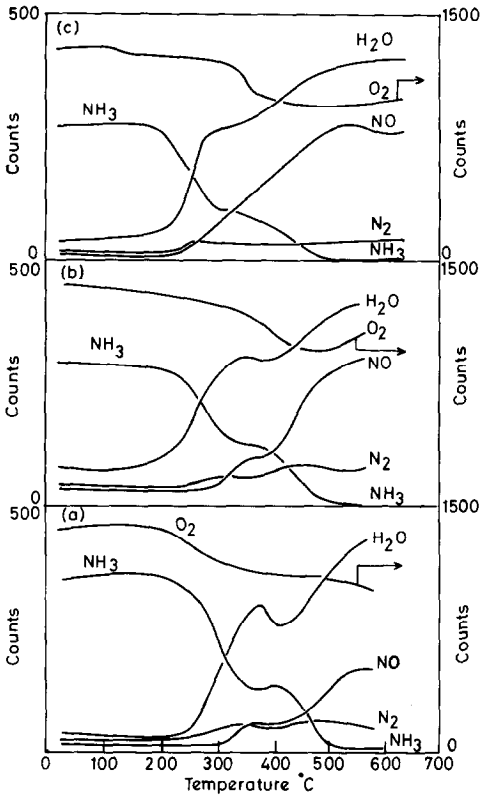

FIG. 4. Thermograms of aerobic oxidation of ammonia over oxygenated (a) 123, (b) Pr123, and (c) 1221 ($NH_3 : O_2 = 1 : 5$). Flow rate of ammonia was 8 μmole/cm^2/s.

Aerobic Oxidation of NH_3

NH_3 and O_2 were premixed in the ratio of 1 : 5 and passed over the catalyst bed. Thermograms of $NH_3 + O_2$ over the catalyst are shown in Figs. 4a, 4b, and 4c for the fully oxygenated 123, Pr123, and 1221, respectively. H_2O and NO were the main products in the case of Pr123 and 1221, but with 123(O), N_2 was also formed. When the reactions were carried out with oxygen-desorbed 123 and 1221 samples, as shown in Figs. 5a and 5b, respectively, NO and H_2O were the products. From the peak intensity of NH_3 and NO, complete conversion of ammonia to NO can be seen with 1221 as catalyst at temperatures above 400°C. In Fig. 6 we show selected X-ray diffraction lines, which are characteristic of the orthorhombic and tetragonal phases of 123 systems. The 123(O) changed to 123(T) after oxygen desorption (curve 6b) and also after anaerobic oxidation of NH_3 (curve 6c). The 123(O) remained orthorhombic under aerobic conditions. Furthermore, the 123(T) became converted to 123(O) even after the complete oxidation of NH_3. In Fig. 7 we show similar patterns for Pr123 and in Fig. 8, we show the variation that occurs in the case of 1221. The cell parameters, cell volume, and the oxygen contents in each of these cases are given in Tables 1–3.

The reaction under anaerobic conditions can be represented as follows, assuming $NO : N_2$ is 1 : 1:

$$11YBa_2Cu_3O_{6.95} + 3NH_3 \rightarrow 11YBa_2Cu_3O_{6.45} + \tfrac{9}{2}H_2O + N_2 + NO. \quad (5)$$

However, under aerobic conditions, the reaction is

$$2NH_3 + \tfrac{5}{2}O_2 \xrightarrow{YBa_2Cu_2CoO_{7.15}} 2NO + 3H_2O. \quad (6)$$

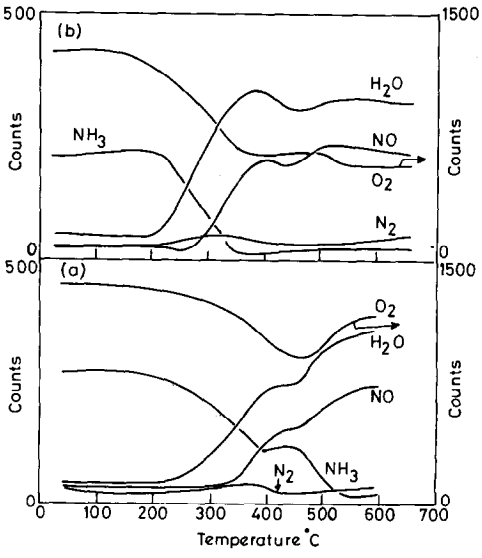

FIG. 5. Thermograms of aerobic oxidation of NH_3 over oxygen-desorbed samples (a) 123 and (b) 1221 ($NH_3 : O_2 = 1 : 5$). Flow rate of ammonia was 10 μmole/cm^2/s.

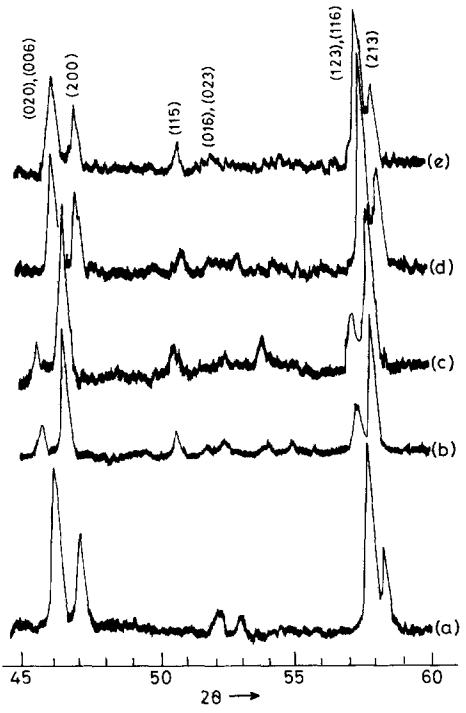

FIG. 6. Selected X-ray diffraction lines of the catalysts: (a) 123(O); (b) oxygen-desorbed 123; (c) 123(O)/NH_3/TPR; (d) 123(O)/NH_3 + O_2(1 : 5)/TPR; and (e) 123(O)/NH_3 + O_2(1 : 5)/370°C.

Thus, under aerobic conditions, 123(T) as well as 1221 acts as a catalyst for Reaction (6). From the relative intensity of NH_3, NO, and H_2O mass peaks, we see that almost 100% conversion occurs at temperatures above 400°C (see Fig. 5b) for an ammonia flow rate of 10 μmole/cm^2/s over 0.3 g of the catalyst. Kinetics of the reaction and conversion rates for higher flow rates over catalysts of higher surface area need to be investigated. When oxygen-desorbed samples were used as catalysts, the products were H_2O and NO under aerobic conditions and the catalysts were oxygenated. Thus the incorporation of oxygen into the structure does occur during the reaction. Since we see the transformation of 123(O) to 123(T) as NH_3 is passed over the catalyst, oxygen atoms in the chain Cu are selectively utilised for the reaction.

The Co-substituted 1221 compound is a special case. $YBa_2Cu_2CoO_{7.26}$ is reduced to $YBa_2Cu_2CoO_{7.02}$ when NH_3 is passed over the catalyst. This compound remains tetragonal even after the removal of oxygen in excess of 7. Since the 1221 structure remains intact after the NH_3 oxidation to H_2O and NO, an excess of 7 oxygen from the *a*/2 or *b*/2 lattice position is utilized in the oxidation reaction. The higher reactivity of the Co-substituted compound can then be attributed to the involvement of Co ion in a higher oxidation state, such as Co^{4+}. From our studies, we suggest that holes in this compound as given in Eq. (4) is responsible for NO specificity. The NH_3 oxidation is NO specific over $La_{1-x}Sr_xCoO_3$ (*24*) wherein Co^{4+} presence is well recognized (*23–25*).

CONCLUSIONS

(a) The activation energy values for oxygen desorption from 123, Pr123, and Co-substituted 1221 are 28.2, 26.4, and 22.3 kcal/mol, respectively.

(b) Anaerobic oxidation of NH_3 over 123,

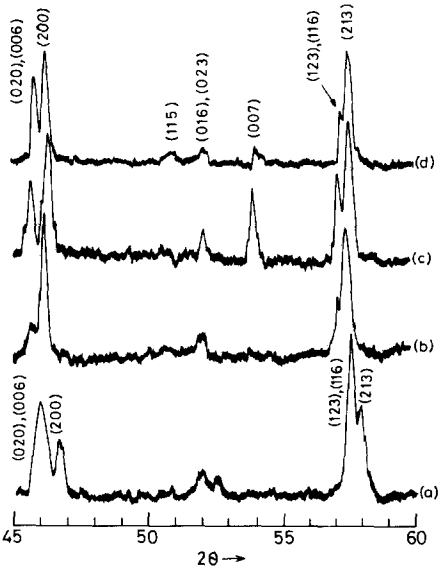

FIG. 7. Selected X-ray diffraction lines of the catalysts: (a) Pr123(O); (b) Pr123(T) oxygen desorbed; (c) Pr123/NH_3/TPR; and (d) Pr123(O)/NH_3 + O_2 (1 : 5)/TPR.

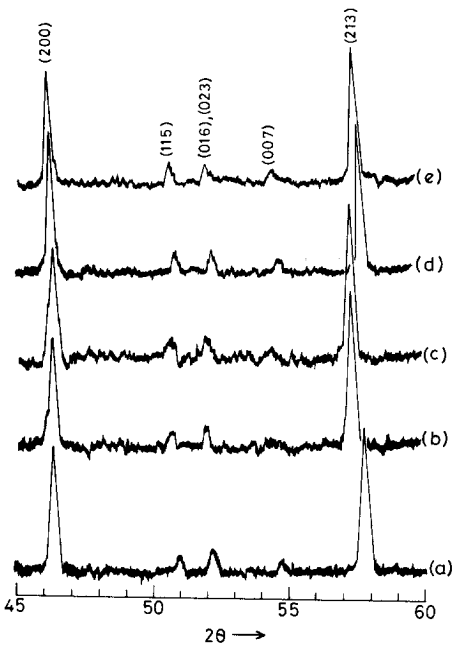

FIG. 8. Selected X-ray diffraction lines of the catalyst (a) $YBa_2Cu_2CoO_{7+x}$ (1221); (b) 1221 oxygen desorbed; (c) 1221/NH_3/TPR; (d) 1221/NH_3 + O_2(1 : 5)/TPR; and (e) 1221 (oxygen desorbed)/NH_3 + O_2(1 : 5)/TPR.

Pr123, and 1221 shows the products as H_2O, N_2, and NO and the oxides were transformed to tetragonal phases.

(c) The reactivity of the oxygen associated with the chain Cu is not altered when Y ion is substituted by Pr ion even though the latter compound is nonsuperconducing.

(d) Aerobic oxidation of NH_3 is NO specific over all the three catalysts and the Co-substituted 1221 is the most stable catalyst for this reaction. NH_3 to NO conversion was nearly total when oxygen-desorbed samples of 123 and 1221 were used at a flow rate of 10 μmole/cm^2/s.

(e) The presence of holes in the Co ion in the form $Co^{4+}O^{2-} \rightleftarrows Co^{3+}O^-$ is suggested to be responsible for the higher reactivity of $YBa_2Cu_2CoO_{7+x}$.

ACKNOWLEDGMENTS

The authors thank Professor C. N. R. Rao for encouragement. Discussions with Professor J. Gopalakrishnan have been very useful. We thank Mr. G. S. Ramesh for setting up the data acquisition system.

REFERENCES

1. Wu, M. K., Ashburn, J. R., Torng, C. J., Hor, P. H., Meng, R. L., Gao L., Huang, Z. H., Wang, Y. Q., and Chu, C., W., *Phys. Rev. Lett.* **58,** 908 (1987).
2. Tarascon, J. M., Barboux, P., Bagley, B. G., Greene, L. H., McKinnon, W. R., and Hull, G. W., *ACS Symp,* 198 (1987).
3. Jorgenson, J. D., Veal, B. W., Paulikas, A. P., Nowicki, L. J., Crabtree, G. W., Clauss, H., and Kwok, W. K., *Phys. Rev B* **41,** 1863 (1989).
4. Rao, C. N. R., *J. Solid State Chem.* **74,** 147 (1988).
5. Hegde, M. S., *Mater. Res. Bull.* **23,** 1171 (1988).
6. Kitson, M., and Lambert, R. M., *Surf. Sci.* **109,** 60 (1981).
7. Hansen, S., Otamiri, J., Bovin, J.-O., and Andersson, A., *Nature* **334,** 14 (1988); Hansen, S., Otamini, J. C., and Andersson, A., *Catal. Lett.* **6,** 33 (1990).
8. Salvador, P., *J. Phys. Chem.* **93,** 8278 (1989).
9. Mizuno, N., Yamato, M., and Misono, M., *J. Chem. Soc. Chem. Commun.,* 887 (1988).
10. Halasz, I., Brenner, A., Shelef, M., and Simon Ng, K. Y., *J. Catal.* **126,** 109 (1990).
11. Solderholm, L., Zhang, K., Hinks, D. G., Beno, M. A., Jorgenson, J. D., Segre, C. V., and Shuller, I. K., *Nature* **328,** 604 (1987).
12. Tarascon, J. M., Barboux, P., Miceli, P. F., Greene, L. H., and Hull, G. W., *Phys. Rev B* **37,** 7458 (1988).
13. Ganguly, A. K., Rao, C. N. R., Sequeira, A., and Rajagopal, H., *Z. Phys. B: Condens. Matter* **74,** 215 (1989).
14. Kebede, A., Jee, C. S., Schwegler, J., Crow, J. E., Mihalisin, T., Myer, G. H., Salomon, R. E., Schlottmann, P., Kuric, M. V., Bloom, S. H., and Guestin, R. P., *Phys. Rev B* **40,** 4453 (1989).
15. Harris, D. C., and Hewston, T. A., *J. Solid State Chem.* **69,** 182 (1987).
16. Dawson, P. T., and Wallace, P. C., *in* "Experimental Methods in Catalytic Research" (R. B. Anderson and P. T. Dawson, Eds.), P. 211. Academic Press, New York, 1976.
17. Goodenough, J. B., and Manthiram, A., *J. Solid State Chem.* **88,** 115 (1990).
18. Au, C. T., and Roberts, M. W., *Nature* **319,** 206 (1986).
19. Tao, Y. K., Swinnea, J. S., Manthiram, A., Kim, J. S., Goodenough, J. B., and Steinfink, H., *J. Mater. Res.* **3,** 248 (1988).
20. O'Keeffe, M., and Hansen, S., *J. Am. Chem. Soc.* **110,** 1506 (1988).
21. Miceli, P. F., Tarascon, J. M., Greene, L. H., Barboux, P., Rotella, F. J., and Jorgensen, J. D., *Phys. Rev B* **37,** 5932 (1988).

22. Gopalakrishnan, J., Subramanian, M. A., and Sleight, A. W., *J. Solid State Chem.* **80,** 156 (1989).
23. Zhang, H. M., Shimizu, Y., Teraoka, Y., Miura, N., and Yamazoe, N., *J. Catal.* **121,** 432, (1990).
24. Wu, Y., Yu, T., Dou, B.-S., Wang, C.-X., Xie, X.-F., Yu, Z.-L., Fan, S.-R., Fan, Z.-R., and Wang, L.-C., *J. Catal.* **120,** 88 (1989).
25. Ganguly, P., and Hegde, M. S., *Phys. Rev. B* **37,** 5107 (1988).